RANDOM VIBRATION OF SHEAR DEFORMABLE FGM PLATES

Vedat Dogan

RANDOM VIBRATION OF SHEAR DEFORMABLE FGM PLATES

VEDAT DOGAN

In this research, the vibration of the functionally graded material (FGM) plates under random excitation is presented. The FGM plate is assumed to be moderately thick. One of the refined plate theories, the first-order shear deformable theory (FSDT) is adopted to account for the transverse shear strain. The refined form of shear correction factor is used. The plate is assumed to be simply supported along all edges with movable ends. The mechanical properties of the FGM plate are graded in the thickness direction only according to a simple power-law distribution in terms of volume fraction of constituents. Mechanical properties of constituents (ceramic and metal) of the FGM plate are assumed temperature-dependent. The FGM plate is subjected to the random pressure that is considered as a stationary and homogenous random process with zero mean and Gaussian distribution. Both the spectral density method and Monte Carlo method are used for the linear responses. Thermal effects are only included in the Monte Carlo method. The root mean square (RMS) and mean responses of the FGM plate for different plate sizes, sound pressure levels, volume fractions and temperature distributions are presented.

1. Introduction

Functionally graded materials (FGMs) are advanced inhomogeneous composite materials. The compositions of the constituents of FGMs vary smoothly and continuously in certain directions (particularly in the thickness direction), and consequently, the FGMs eliminate the interface problems such as cracks and stress concentrations encountered in the traditional laminated composite plates. FGM plates are typically made of a metal and ceramic mixture and used as structural elements in high-temperature environments.

The FGMs have attracted the considerable attention of many researchers since they were first developed in Japan three decades ago [Koizumi 1997]. To the present, extensive research has been conducted on the dynamic, static, buckling, vibration and thermal stress analysis of FGM plates. Among them, Praveen and Reddy [1998] analyzed the static and dynamic response of FGM plates by using the first-order shear deformation theory (FSDT) and the von Karman strains. The stresses and deflections of the FGM plates are examined under mechanical and thermal loadings. They found that grading of material properties is very important for the plate responses. Reddy [2000] presented a formulation for the simply supported FGM plates based on the third-order shear deformation theory and developed the associated finite element model, which includes thermomechanical coupling and geometric nonlinearities. Praveen, Chin and Reddy [Praveen et al. 1999] investigated the response of FGM cylinders to rapid heating of the inner surface with temperature-dependent material properties. The finite element formulation and axisymmetric heat equation are used. The temperature and radial/hoop stress distributions versus radial distance due to rapid heating are reported. Alijani, Bakhtiari and Amabili [Alijani et al. 2011] analyzed the nonlinear vibrations of simply supported moderately thick FGM plates in a thermal environment by

using the first-order shear deformation theory. Zhang, Hao, Guo and Chen [Zhang et al. 2012] investigated the nonlinear responses of FGM plates subjected to combined in-plane and transverse excitations by using Reddy's third-order plate theory. They found that the nonlinear responses of the FGM plates are more sensitive to transverse excitation.

Effects of the micromechanics Voigt and Moni–Tanaka models on the vibration responses of FGM plates are investigated by Shen and Wang [2012]. They used a high-order shear deformation plate theory to develop the governing equations. Since the differences between two micromechanics models were small, the Voigt model can be reasonable for finding the responses of FGM plates and shells. Nguyen-Xuan, Tran, Thai and Nguyen-Thoi [Nguyen-Xuan et al. 2012] presented a finite element approach for analysis of FGM plates subjected to mechanical and thermal loading. This method is applied in several static/dynamic problems of FGM plates.

Hosseini and Fazelzadeh [2010] presented the nonlinear vibration and the aerothermoelastic postcritical analysis of the FGM panels in a supersonic airflow. Temperature-dependent material properties are considered, and the first-order piston theory is used for the aerodynamics loading. Prakash, Singha and Ganapathi [Prakash et al. 2012] investigated the nonlinear vibration of the FGM plates by a shear flexible finite element approach. The FGM plate is modeled with the FSDT, and third-order piston theory is employed for the aerodynamics loading.

Zhao, Lee and Liew [Zhao et al. 2009] examined the mechanical and thermal buckling behavior of the FGM plates using the element-free kp-Ritz method. Solid plates and plates with holes are analyzed. It was determined that the hole size and volume fraction greatly influenced the buckling loads and modes. Hosseini-Hashemi, Taher, Akhavan and Omidi [Hosseini-Hashemi et al. 2010] analyzed the free vibration of the moderately thick FGM plates on elastic foundations by using the FSDT. Parametric studies regarding the elastic foundation stiffness, aspect ratios, gradient indices and thickness to length ratios are conducted. Ghannadpour, Ovesy and Nassirnia [Ghannadpour et al. 2012] presented a finite strip method for analyzing the thermal buckling of the FGM plate. The classical plate theory (CPT) is used for the formulations, and three types of thermal loadings are considered. Mohammadi, Saidi and Jomehzadeh [Mohammadi et al. 2010] studied the Levy solution for the mechanical buckling of the FGM plate based on the CPT. Thai and Choi [2012] presented a refined shear deformation theory, which is used for free vibration analysis of FGM plates on Pasternak-type foundation. Closed-form solutions for natural frequency with different boundary conditions are obtained and compared to the natural frequencies found in the literature. Dynamic, bending, thermal and vibration analysis of FGM plates by using different-order plates theories are conducted by H.-S. Shen and his associates [Yang and Shen 2003; 2002; Huang and Shen 2004]. Extensive nonlinear analysis of shear deformable FGM plates and shell can be found in [Shen 2009].

Hasheminejad and Gheshlaghi [2012] studied the transient vibration of thick FGM plates resting on the elastic foundations under blast and moving loads using the linear elasticity theory. Yang and Gao [2013] studied dynamic stress analysis of the FGM plates with a circular hole under an in-plane compressive load at infinity. Fakhari, Ohadi and Yousefian [Fakhari et al. 2011] investigated the vibrations of FGM plates with piezoelectric layers under thermal, electrical and mechanical loadings. They used the finite element method based on HSDT with geometric nonlinearity. Elishakoff and Gentilini [2005] developed a three-dimensional linear elasticity solution using the Ritz minimum energy principle for the FGM plates with all edges clamped. Mantari and Soares [2012] analytically analyzed the bending of the FGM plates by using a newly developed HSDT. Comparison studies are carried out to validate the present theory.

Lee, Zhao and Reddy [Lee et al. 2010] analyzed the postbuckling behavior of the FGM plates under mechanical in-plane edge compressive and thermal loading by using the element-free kp-method. The FSDT and von Karman–type nonlinearity are employed.

In the present study, the linear vibration of the functionally graded material (FGM) plates under random excitation is presented. One of the shear deformable plate theories, FSDT, is employed for the formulation. A modified shear correction factor is used to take into account the transverse shear strain effects. It is assumed that the FGM plate is simply supported with movable edges. The FGM plates are considered as ceramic–metal mixtures whose mechanical properties vary exponentially through the thickness only. Temperature dependency of mechanical properties of the constituents are also taken into account for the random vibration in the thermal environment. Two approaches are used for random responses in this study. The first approach is based on the normal mode method to determine the spectral density of the response, and the second approach is based on the Monte Carlo simulation of the external random pressure, the multimode Galerkin technique and the numerical integration procedure. The temperature effect is taken into account only in the second approach.

2. Structural formulation

The equations of motion of an FGM plate shown in Figure 1 using the first-order shear deformation theory (FSDT) in terms of the mid-plane displacements $u_0(x, y, t)$, $v_0(x, y, t)$ and $w_0(x, y, t)$ in the x, y and z directions, respectively, and the rotations $\phi_x(x, y, t)$ and $\phi_y(x, y, t)$ of the transverse normal about the y and x axes, respectively, can be written as [Reddy 2004]

$$A_{11}u_{0,xx} + A_{12}v_{0,xy} + B_{11}\phi_{x,xx} + B_{12}\phi_{y,yy} + A_{66}(u_{0,yy} + v_{0,yx})$$
$$+ B_{66}(\phi_{x,yy} + \phi_{y,yx}) - N_{xx,x}^T = I_0(\ddot{u}_0 + c\dot{u}_0) + I_1(\ddot{\phi}_x + c\dot{\phi}_x), \quad (1)$$

$$A_{22}v_{0,yy} + A_{12}u_{0,yx} + B_{22}\phi_{y,yy} + B_{12}\phi_{x,yx} + A_{66}(u_{0,xy} + v_{0,xx})$$
$$+ B_{66}(\phi_{x,xy} + \phi_{y,xx}) - N_{yy,y}^T = I_0(\ddot{v}_0 + c\dot{v}_0) + I_1(\ddot{\phi}_y + c\dot{\phi}_y), \quad (2)$$

$$\kappa A_{55}(w_{0,xx} + \phi_{x,x}) + \kappa A_{44}(w_{0,yy} + \phi_{y,y}) + \theta(w_0) + p^r(x, y, t) = I_0(\ddot{w}_0 + c\dot{w}_0), \quad (3)$$

$$B_{11}u_{0,xx} + B_{12}v_{0,xy} + D_{11}\phi_{x,xx} + D_{12}\phi_{y,xy} + B_{66}(u_{0,yy} + v_{0,xy})$$
$$+ D_{66}(\phi_{x,yy} + \phi_{y,yx}) - \kappa A_{55}(w_{0,x} + \phi_x) - M_{xx,x}^T = I_2(\ddot{\phi}_x + c\dot{\phi}_x) + I_1(\ddot{u}_0 + c\dot{u}_0), \quad (4)$$

$$B_{22}v_{0,yy} + B_{12}u_{0,xy} + D_{22}\phi_{y,yy} + D_{12}\phi_{x,yx} + B_{66}(u_{0,yx} + v_{0,xx})$$
$$+ D_{66}(\phi_{x,xy} + \phi_{y,xx}) - \kappa A_{44}(w_{0,y} + \phi_y) - M_{yy,y}^T = I_2(\ddot{\phi}_y + c\dot{\phi}_y) + I_1(\ddot{v}_0 + c\dot{v}_0), \quad (5)$$

where

$$\theta(w_0) = (N_{xx}w_{0,x} + N_{xy}w_{0,y})_{,x} + (N_{xy}w_{0,x} + N_{yy}w_{0,y})_{,y} \quad (6)$$
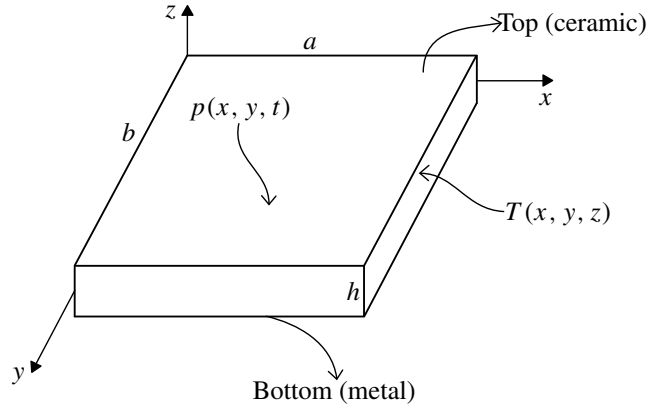
with

$$N_{xx}(x, y, t) = A_{11}u_{0,x} + A_{12}v_{0,y} + B_{11}\phi_{x,x} + B_{12}\phi_{y,y} - N_{xx}^T, \quad (7)$$

$$N_{yy}(x, y, t) = A_{12}u_{0,x} + A_{22}v_{0,y} + B_{12}\phi_{x,x} + B_{22}\phi_{y,y} - N_{yy}^T, \quad (8)$$

$$N_{xy}(x, y, t) = A_{66}(u_{0,y} + v_{0,y}) + B_{66}(\phi_{x,y} + \phi_{y,x}), \quad (9)$$

in which a subscript comma denotes the partial derivative with respect to the indicated coordinates and

Figure 1. Shear deformable FGM plate geometry, loading and coordinate system.

time t, κ is the shear correction factor, $p^r(x, y, t)$ is the random pressure, c is the viscous damping coefficient and I_0, I_1 and I_2 are the mass inertias defined as

$$(I_0, I_1, I_2) = \int_{-h/2}^{h/2} \rho(z, T) \cdot (1, z, z^2) \, dz, \tag{10}$$

in which ρ is the mass density and h is the thickness of the FGM plate. Furthermore,

$$(A_{ij}, B_{ij}, D_{ij}) = \int_{-h/2}^{h/2} Q_{ij} \cdot (1, z, z^2) \, dz, \quad i, j = 1, 2, 6, \tag{11}$$

$$A_{ij} = \int_{-h/2}^{h/2} Q_{ij} \, dz, \qquad i, j = 4, 5, \tag{12}$$

where

$$Q_{11} = Q_{22} = \frac{E(z, T)}{1 - \nu^2(z, T)}, \qquad Q_{12} = \frac{\nu(z, T) E(z, T)}{1 - \nu^2(z, T)},$$

$$Q_{16} = Q_{26} = 0, \qquad Q_{44} = Q_{55} = Q_{66} = \frac{E(z, T)}{2[1 + \nu(z, T)]}, \tag{13}$$

where the elasticity modulus $E(z, T)$, the density of the plate $\rho(z, T)$, Poisson's ratio $\nu(z, T)$ and the thermal expansion coefficient $\alpha(z, T)$ are all assumed to be functions of temperature T and coordinate z in the thickness direction according to a power law distribution as [Praveen and Reddy 1998; Reddy 2000; Shen 2009]

$$E(z, T) = (E_t(T) - E_b(T))\left(\frac{2z + h}{2h}\right)^n + E_b(T), \tag{14}$$

$$\rho(z, T) = (\rho_t(T) - \rho_b(T))\left(\frac{2z + h}{2h}\right)^n + \rho_b(T), \tag{15}$$

$$\nu(z, T) = (\nu_t(T) - \nu_b(T))\left(\frac{2z + h}{2h}\right)^n + \nu_b(T), \tag{16}$$

$$\alpha(z, T) = (\alpha_t(T) - \alpha_b(T))\left(\frac{2z + h}{2h}\right)^n + \alpha_b(T), \tag{17}$$
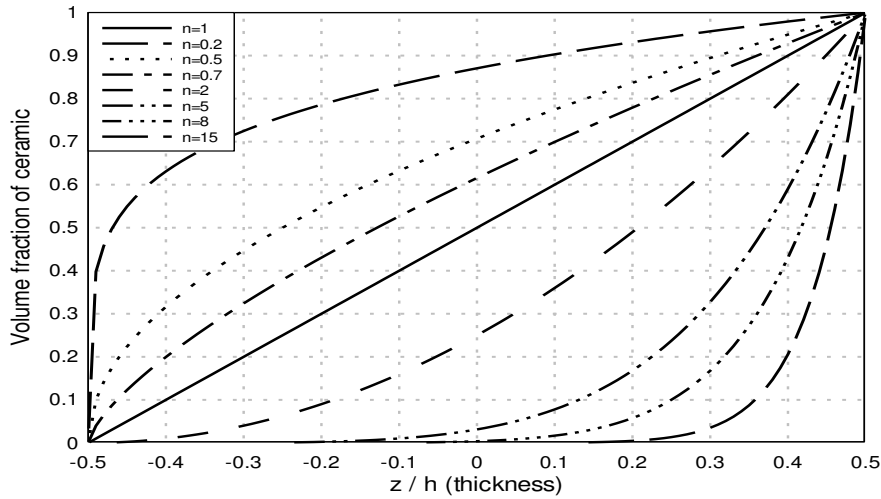
Figure 2. Volume fraction of ceramic through the thickness for the different volume
fraction n.

where subscripts t and b denote the top and bottom of the plate and n is the material distribution parameter.
When the material distribution parameter n increases, the volume fraction of ceramic diminishes and
the FGM plate becomes more metal-rich as shown in Figure 2. The temperature dependent material
properties $P(T)$ of the constituents of the FGM plate can be expressed by [Reddy and Chin 1998]

$$P(T) = P_0(P_{-1}T^{-1} + 1 + P_1T + P_2T^2 + P_3T^3), \tag{18}$$

where P_0, P_{-1}, P_1, P_2 and P_3 are the coefficients of temperature T (in K) in the cubic fit of the material
property and are unique to the materials.

The shear correction factor for an FGM plate can be defined as [Efraim and Eisenberger 2007; Efraim
2011]

$$\kappa(T) = \frac{5}{6 - (\nu_1(T)V_1 - \nu_2(T)V_2)}, \tag{19}$$

where V_1 and V_2 are the volume fractions of constituents in the whole cross-section.

In this study, a simply supported FGM plate with movable ends is considered. For an FSTD plate, the
boundary conditions are given as follows. At $x = 0, a$,

$$v_0(x, y, t) = w_0(x, y, t) = \phi_y(x, y, t) = 0, \tag{20}$$

$$N_{xx}(x, y, t) = A_{11}u_{0,x} + A_{12}v_{0,y} + B_{11}\phi_{x,x} + B_{12}\phi_{y,y} - N_{xx}^T = 0, \tag{21}$$

$$M_{xx} = B_{11}u_{0,x} + B_{12}v_{0,y} + D_{11}\phi_{x,x} + D_{12}\phi_{y,y} - M_{xx}^T = 0. \tag{22}$$

At $y = 0, b$,

$$u_0(x, y, t) = w_0(x, y, t) = \phi_x(x, y, t) = 0, \tag{23}$$

$$N_{yy}(x, y, t) = A_{12}u_{0,x} + A_{22}v_{0,y} + B_{12}\phi_{x,x} + B_{22}\phi_{y,y} - N_{yy}^T = 0, \tag{24}$$

$$M_{yy} = B_{12}u_{0,x} + B_{22}v_{0,y} + D_{12}\phi_{x,x} + D_{22}\phi_{y,y} - M_{yy}^T = 0, \tag{25}$$

where the thermal force and moment resultants are

$$\left(\begin{Bmatrix} N_{xx}^T \\ N_{yy}^T \\ N_{xy}^T \end{Bmatrix}, \begin{Bmatrix} M_{xx}^T \\ M_{yy}^T \\ M_{xy}^T \end{Bmatrix} \right) = \int_{-h/2}^{h/2} \begin{Bmatrix} (Q_{11} + Q_{12})\alpha(z, T) \\ (Q_{12} + Q_{22})\alpha(z, T) \\ 0 \end{Bmatrix} \cdot \Delta T(x, y, z) \cdot (1, z)\, dz, \tag{26}$$

where ΔT is the temperature change from a stress-free state.

3. Solution procedure

For undamped free vibration analysis, by setting all mechanical and thermal loads to zero, it can be shown that the following functions satisfy the boundary conditions (20)–(25) [Reddy 2000]:

$$u_0(x, y, t) = \widehat{U} \cos(\alpha_m x) \sin(\beta_n y) e^{i\omega t}, \tag{27}$$

$$v_0(x, y, t) = \widehat{V} \sin(\alpha_m x) \cos(\beta_n y) e^{i\omega t}, \tag{28}$$

$$w_0(x, y, t) = \widehat{W} \sin(\alpha_m x) \sin(\beta_n y) e^{i\omega t}, \tag{29}$$

$$\phi_x(x, y, t) = \widehat{X} \cos(\alpha_m x) \sin(\beta_n y) e^{i\omega t}, \tag{30}$$

$$\phi_y(x, y, t) = \widehat{Y} \sin(\alpha_m x) \cos(\beta_n y) e^{i\omega t}, \tag{31}$$

where

$$\alpha_m = \frac{m\pi}{a} \quad \text{and} \quad \beta_n = \frac{n\pi}{b}. \tag{32}$$

By substituting (27)–(31) into the equations of motion, (1)–(5), one can obtain

$$([K] - \omega^2[M])\{\psi\} = 0, \tag{33}$$

where

$$\{\psi\} = \{\widehat{U}, \widehat{V}, \widehat{W}, \widehat{X}, \widehat{Y}\}^T \tag{34}$$

and $[K]$ and $[M]$ are the stiffness and mass matrices, and ω is the natural frequency of the vibration. Elements of the stiffness and mass matrices are given in Appendix A.

For each (m, n), there are five natural frequencies ω_{mni}^2 and corresponding natural modes $\{\widehat{U}_{mni}, \widehat{V}_{mni}, \widehat{W}_{mni}, \widehat{X}_{mni}, \widehat{Y}_{mni}\}^T$ $(i = 1, 2, 3, 4, 5)$.

Random vibration.

Isothermal case. For the random forced vibration without thermal effect, the responses are expanded in terms of natural modes [Cederbaum et al. 1992; Elishakoff 1999]

$$u_0(x, y, t) = \sum_m \sum_n \sum_{i=1}^{5} U_{mni}(x, y) q_{mni}(t), \tag{35}$$

$$v_0(x, y, t) = \sum_m \sum_n \sum_{i=1}^{5} V_{mni}(x, y) q_{mni}(t), \tag{36}$$

$$w_0(x, y, t) = \sum_m \sum_n \sum_{i=1}^{5} W_{mni}(x, y) q_{mni}(t), \tag{37}$$

$$\phi_x(x, y, t) = \sum_m \sum_n \sum_{i=1}^5 X_{mni}(x, y)q_{mni}(t), \qquad (38)$$

$$\phi_y(x, y, t) = \sum_m \sum_n \sum_{i=1}^5 Y_{mni}(x, y)q_{mni}(t), \qquad (39)$$

where

$$U_{mni}(x, y) = \widehat{U}_{mni} \cos(\alpha_m x) \sin(\beta_n y), \qquad (40)$$
$$V_{mni}(x, y) = \widehat{V}_{mni} \sin(\alpha_m x) \cos(\beta_n y), \qquad (41)$$
$$W_{mni}(x, y) = \widehat{W}_{mni} \sin(\alpha_m x) \sin(\beta_n y), \qquad (42)$$
$$X_{mni}(x, y) = \widehat{X}_{mni} \cos(\alpha_m x) \sin(\beta_n y), \qquad (43)$$
$$Y_{mni}(x, y) = \widehat{Y}_{mni} \sin(\alpha_m x) \cos(\beta_n y) \qquad (44)$$

by introducing (35)–(39) into (1)–(5); and using free vibration analysis and orthogonality of eigenmodes, one can obtain

$$\ddot{q}_{mni} + 2\xi_{mni}\omega_{mni}\dot{q}_{mni} + \omega_{mni}^2 q_{mni} = Q_{mni}^r, \qquad (45)$$

where

$$2\xi_{mni}\omega_{mni} = c \qquad (46)$$

and the generalized random force

$$Q_{mni}^r(t) = \frac{1}{M_{mni}} \int_0^a \int_0^b p^r(x, y, t) W_{mni}(x, y) \, dx \, dy, \qquad (47)$$

where the generalized mass

$$M_{mni} = \int_0^a \int_0^b \left\{ I_0(U_{mni}^2 + V_{mni}^2 + W_{mni}^2) + 2I_1(X_{mni}U_{mni} + Y_{mni}V_{mni}) + I_2(X_{mni}^2 + Y_{mni}^2) \right\} dx \, dy. \quad (48)$$

By using random vibration theory [Lin 1976; Elishakoff 1999; Maymon 1998], the deflection response spectral density for $w_0(x, y, t)$ can be derived as

$$S_{WW}(x_1, y_1, x_2, y_2, \omega) = \sum_{mni} \sum_{rsj} W_{mni}(x_1, y_1) W_{rsj}(x_2, y_2) H_{mni}(\omega) H_{rsj}^*(\omega) S_{Q_{mni}^r Q_{rsj}^r}(\omega), \qquad (49)$$

where

$$S_{Q_{mni}^r Q_{rsj}^r}(\omega) = \frac{1}{M_{mni}} \frac{1}{M_{rsj}} \int_0^a \int_0^b \int_0^a \int_0^b S_p(x_1, y_1, x_2, y_2, \omega) W_{mni}(x_1, y_1) W_{rsj}(x_2, y_2) \, dx_1 \, dy_1 \, dx_2 \, dy_2 \qquad (50)$$

and

$$H_{mni}(\omega) = \frac{1}{\omega_{mni}^2[\omega_{mni}^2 - \omega^2 + 2i\xi_{mni}\omega_{mni}\omega]}, \qquad (51)$$

and $*$ indicates a complex conjugate. We define

$$R_{WW}(x_1, y_1, x_2, y_2, \tau) = \int_{-\infty}^{\infty} S_{WW}(x_1, y_1, x_2, y_2, \omega)e^{i\omega\tau}\, d\omega. \tag{52}$$

The root mean square (RMS) values of deflection at a point ($x = x_1 = x_2$ and $y = y_1 = y_2$) can be computed from

$$\text{RMS} = \sqrt{\int_{-\infty}^{\infty} S_{ww}(x, y, \omega)\, d\omega}. \tag{53}$$

Thermal case. When thermal effects are included, due to multiplication of thermal terms and deflection terms, a time domain approach is used to develop the solution. For the time domain solution, displacements are expanded into double Fourier series as

$$u_0(x, y, t) = \sum_m \sum_n U_{mn}(t) \cos(\alpha_m x) \sin(\beta_n y), \tag{54}$$

$$v_0(x, y, t) = \sum_m \sum_n V_{mn}(t) \sin(\alpha_m x) \cos(\beta_n y), \tag{55}$$

$$w_0(x, y, t) = \sum_m \sum_n W_{mn}(t) \sin(\alpha_m x) \sin(\beta_n y), \tag{56}$$

$$\phi_x(x, y, t) = \sum_m \sum_n X_{mn}(t) \cos(\alpha_m x) \sin(\beta_n y), \tag{57}$$

$$\phi_y(x, y, t) = \sum_m \sum_n Y_{mn}(t) \sin(\alpha_m x) \cos(\beta_n y), \tag{58}$$

where

$$\alpha_m = \frac{m\pi}{a} \quad \text{and} \quad \beta_n = \frac{n\pi}{b}. \tag{59}$$

Temperature in (26) is also expanded in a double Fourier sine series as

$$T(x, y, z) = \sum_{m=1}\sum_{n=1} T_{mn}(z) \sin(\alpha_m x) \sin(\beta_n y), \tag{60}$$

where

$$T_{mn}(z) = \frac{4}{a \cdot b} \int_0^a \int_0^b T(x, y, z) \sin(\alpha_m x) \sin(\beta_n y)\, dx\, dy. \tag{61}$$

It is also assumed that temperature varies only in the z direction or uniformly throughout the plate. Then the temperature change can be written in the form

$$\Delta T(x, y, z) = \Delta T(z) \sum_m \sum_n \frac{1}{m \cdot n} \sin(\alpha_m x) \sin(\beta_n y), \tag{62}$$

where

$$\Delta T(z) = T(z) - T_0, \tag{63}$$

where T_0 is a stress-free reference temperature ($T_0 = 300\,\text{K}$ is taken).

The following temperature distributions through the thickness (z direction) in (63) are considered. For linear distribution,

$$T(z) = T_b + (T_t - T_b)\left(\frac{2z+h}{2h}\right), \tag{64}$$

where T_b and T_t are the temperatures of the bottom and top of the FGM plate, respectively. For nonlinear distribution of the temperature through the thickness, the heat conduction equation

$$-\frac{d}{dz}\left(k(z)\frac{dT}{dz}\right) = 0 \tag{65}$$

is solved, where the temperature dependency of the thermal conductivity k is not considered. Solution of (65) is carried out by using polynomial series as [Javaheri and Eslami 2002]

$$T(z) = T_b + \frac{T_t - T_b}{C_{tb}}\left[V - \frac{k_{tb}}{(n+1)k_b}V^{n+1} + \frac{k_{tb}^2}{(2n+1)k_b^2}V^{2n+1}\right.$$
$$\left. - \frac{k_{tb}^3}{(3n+1)k_b^3}V^{3n+1} + \frac{k_{tb}^4}{(4n+1)k_b^4}V^{4n+1} - \frac{k_{tb}^5}{(5n+1)k_b^5}V^{5n+1}\right], \tag{66}$$

where

$$C_{tb} = 1 - \frac{k_{tb}}{(n+1)k_b} + \frac{k_{tb}^2}{(2n+1)k_b^2} - \frac{k_{tb}^3}{(3n+1)k_b^3} + \frac{k_{tb}^4}{(4n+1)k_b^4} - \frac{k_{tb}^5}{(5n+1)k_b^5} \tag{67}$$

and

$$V = \frac{2z+h}{2h} \quad \text{and} \quad k_{tb} = k_t - k_b, \tag{68}$$

where k_b and k_t are the thermal conductivity of the bottom and top surfaces of the plate, respectively. Above, n is the material distribution parameter as used in (14)–(17).

The assumed solutions that satisfy the boundary conditions, (20)–(25), are substituted into (1)–(5), then Galerkin's method is employed and the following sets of equations in time domain are obtained:

$$\ddot{U}_{mn} + 2\xi_{mn}\omega_{mn}\dot{U}_{mn} + \frac{I_1}{I_0}(\ddot{X}_{mn} + 2\xi_{mn}\omega_{mn}\dot{X}_{mn})$$
$$+ \frac{1}{I_0}\left(k_{11}U_{mn} + k_{12}V_{mn} + k_{14}X_{mn} + k_{15}Y_{mn} + \bar{N}_{xx}^T\frac{\pi}{n\cdot a}\Big|_{n\,\text{odd}}\right) = 0, \tag{69}$$

$$\ddot{V}_{mn} + 2\xi_{mn}\omega_{mn}\dot{V}_{mn} + \frac{I_1}{I_0}(\ddot{Y}_{mn} + 2\xi_{mn}\omega_{mn}\dot{Y}_{mn})$$
$$+ \frac{1}{I_0}\left(k_{21}U_{mn} + k_{22}V_{mn} + k_{24}X_{mn} + k_{25}Y_{mn} + \bar{N}_{yy}^T\frac{\pi}{m\cdot b}\Big|_{m\,\text{odd}}\right) = 0, \tag{70}$$

$$\ddot{W}_{mn} + 2\xi_{mn}\omega_{mn}\dot{W}_{mn} + \frac{1}{I_0}(k_{33}W_{mn} + k_{34}X_{mn} + k_{35}Y_{mn})$$
$$+ \bar{N}_{xx}^T\sum_{k\,\text{odd}}\sum_{l\,\text{odd}}\sum_{r}\sum_{s}W_{rs}\frac{\alpha_r}{k\cdot l}\xi_1(l,s,n)[\alpha_r\gamma_1(k,r,m) - \alpha_k\gamma_2(k,r,m)]$$
$$+ \bar{N}_{yy}^T\sum_{k\,\text{odd}}\sum_{l\,\text{odd}}\sum_{r}\sum_{s}W_{rs}\frac{\beta_s}{k\cdot l}\gamma_1(k,r,m)[\beta_s\xi_1(l,s,n) - \beta_l\xi_2(l,s,n)] = Q_{mn}(t), \tag{71}$$

$$\ddot{X}_{mn} + 2\xi_{mn}\omega_{mn}\dot{X}_{mn} + \frac{I_1}{I_2}(\ddot{U}_{mn} + 2\xi_{mn}\omega_{mn}\dot{U}_{mn})$$

$$+ \frac{1}{I_2}\left(k_{41}U_{mn} + k_{42}V_{mn} + k_{43}W_{mn} + k_{44}X_{mn} + k_{45}Y_{mn} + \overline{M}_{xx}^T \frac{\pi}{n \cdot a}\Big|_{n \text{ odd}}\right) = 0, \qquad (72)$$

$$\ddot{Y}_{mn} + 2\xi_{mn}\omega_{mn}\dot{Y}_{mn} + \frac{I_1}{I_2}(\ddot{V}_{mn} + 2\xi_{mn}\omega_{mn}\dot{V}_{mn})$$

$$+ \frac{1}{I_2}\left(k_{51}U_{mn} + k_{52}V_{mn} + k_{53}W_{mn} + k_{54}X_{mn} + k_{55}Y_{mn} + \overline{M}_{yy}^T \frac{\pi}{m \cdot a}\Big|_{m \text{ odd}}\right) = 0, \qquad (73)$$

where the generalized random load

$$Q_{mn}(t) = \frac{4}{a \cdot b \cdot I_0} \int_0^a \int_0^b p^r(x, y, t) \sin(\alpha_m x) \sin(\beta_n y) \, dx \, dy \qquad (74)$$

the coefficients γ_1, γ_2, ξ_1 and ξ_2 are given in Appendix B and

$$\left(\left\{\begin{matrix}\overline{N}_{xx}^T \\ \overline{N}_{yy}^T \\ \overline{N}_{xy}^T\end{matrix}\right\}, \left\{\begin{matrix}\overline{M}_{xx}^T \\ \overline{M}_{yy}^T \\ \overline{M}_{xy}^T\end{matrix}\right\}\right) = \int_{-h/2}^{h/2} \left\{\begin{matrix}(Q_{11} + Q_{12})\alpha(z, T) \\ (Q_{12} + Q_{22})\alpha(z, T) \\ 0\end{matrix}\right\} \cdot \Delta T(z) \cdot (1, z) \, dz. \qquad (75)$$

In order to solve (69)–(73), the random pressure is first simulated in the space-time domain and then the generalized random load in (74) is evaluated numerically. The integration can be carried out in a closed form for some special cases. In this study, uniformly distributed random pressure is considered.

4. Numerical examples and discussion

A moderately thick square FGM plate shown in Figure 1 is considered in this section. The square plate has a length of $a = b = 0.5\,\text{m}$ and a thickness of $h = 0.025\,\text{m}$. The FGM plate is assumed to be simply supported with movable edges. First nine modes are retained in the serial expansion to estimate the deflection responses. Deflection responses are computed at the center of the plate (i.e., $x = a/2$ and $y = b/2$). The plate is made of the functionally graded material that is a mixture of the material combination of zirconia (ZrO$_2$) and titanium alloy (Ti-6Al-4V). Temperature-dependent material properties of these constituents are presented in Table 1 and used in (18).

Materials	Property	P_0	P_{-1}	P_1	P_2	P_3
Zirconia	E	244.27×10^9	0	-1.371×10^{-3}	1.214×10^{-6}	-3.681×10^{-10}
	ν	0.2882	0	-1.133×10^{-4}	0	0
	α	12.766×10^{-6}	0	-1.491×10^{-3}	1.006×10^{-5}	-6.778×10^{-11}
	ρ	5700	0	0	0	0
Ti-6Al-4V	E	122.56×10^9	0	-4.586×10^{-4}	0	0
	ν	0.2884	0	1.121×10^{-4}	0	0
	α	7.5788×10^{-6}	0	6.638×10^{-4}	-3.147×10^{-6}	0
	ρ	4429	0	0	0	0

Table 1. Temperature-dependent material properties of ceramic (zirconia) and metal (titanium) [Praveen et al. 1999; Shen 2009; Reddy and Chin 1998].
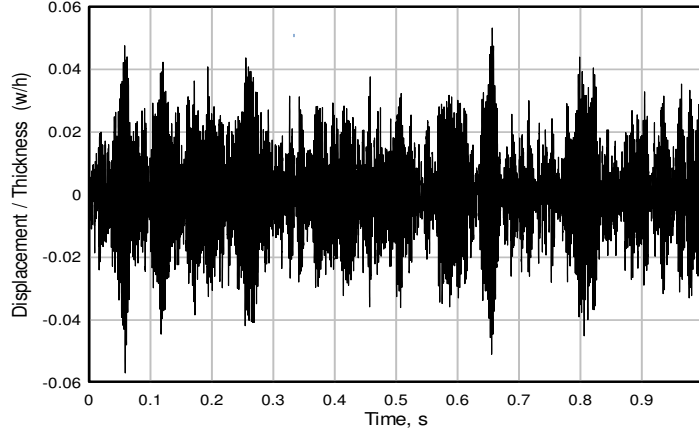
Figure 3. Displacement time histories for uniform random pressure (SPL $= 160$ dB and $n = 0.7$).

The random pressure acting on the top of the plate (ceramic-rich part) is simulated by using the Monte Carlo simulation technique. Uniformly distributed stationary Gaussian random pressure can be simulated as [Shinozuka and Jan 1972]

$$p^r(t_q) = \text{Re}\left[\sum_{r=0}^{M-1} A_r e^{i\phi_r} e^{i\omega_r t_q}\right], \tag{76}$$

where the ϕ_r are independent random phase angles uniformly distributed between 0 and 2π, the ω_r are the frequencies at which the values of spectral density are selected, $M = 2^m$ is the number of simulated points in time, m is a positive integer, $t_q = q\,\Delta t$, where Δt is time interval and $q = 0, 1, 2, \ldots, M-1$, and

$$A_r = [2S_p(\omega)\Delta\omega]^{1/2}, \tag{77}$$

where S_p is the spectral density corresponding to random pressure and $\Delta\omega$ is the frequency bandwidth. The spectral density of the random pressure that is considered uniformly distributed stationary truncated Gaussian white noise is

$$S_p = \begin{cases} S_0 & \text{for } 0 \leq \omega \leq \omega_u, \\ 0 & \text{otherwise,} \end{cases} \tag{78}$$

where S_0 represents random loading intensities, ω is the frequency and ω_u is the upper cut-off frequency. The random load intensities are expressed as

$$S_0 = \begin{cases} \dfrac{p_0^2}{\Delta\omega} 10^{\text{SPL}/10} & \text{for } 0 \leq \omega \leq \omega_u, \\ 0 & \text{otherwise,} \end{cases} \tag{79}$$

where p_0 is the reference pressure ($p_0 = 2 \times 10^{-5}$ Pa) and SPL is the sound pressure level expressed in decibels.

In the numerical examples, the random pressure is simulated by using $M = 32768$, $\Delta t = 0.0000305$ s, $\omega_u = 2\pi \times 8192$ rad/s and $\Delta\omega = 2\pi$ rad/s.
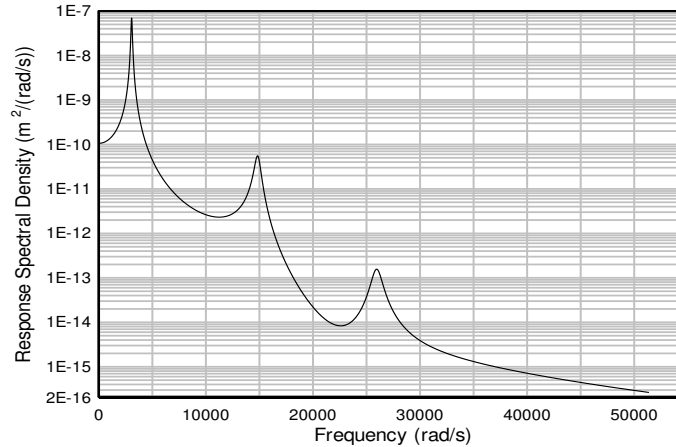
Figure 4. Spectral density of deflection response under random pressure of SPL $=$ 160 dB ($n = 0.7$).

Figure 3 shows the midpoint deflection response history of the FGM plate for SPL $=$ 160 dB without a temperature effect (i.e., at a reference temperature of $T_0 = 300$ K). The random response peak can reach $w_{\max}/h = 0.053$ at $t = 0.65$ s and $w_{\min}/h = -0.056$ at $t = 0.058$ s; and "the average values" of the responses are RMS$/h = 0.00148$ and MEAN$/h \cong 0$. It is evident that the plate vibrates about the plate neutral position since the random input pressure has a Gaussian distribution with zero mean.

The spectral density of the deflection response is displayed in Figure 4. This figure is plotted using (49). There are three peaks that correspond to four natural frequencies of $\omega_{11} = 3048$ rad/s, $\omega_{13} = \omega_{31} = 14816$ rad/s and $\omega_{33} = 25911$ rad/s. Even modes do not contribute to the response at the midpoint since the plate is a square. To demonstrate the contribution of different modes to the RMS response, the area under S_{WW} (as in (53)) is plotted in Figure 5 by integrating the curve in Figure 4 in the frequency domain. It is clear that contribution of the higher modes is very small since the area is not notably increased by increased frequencies beyond the fundamental frequency ω_{11}.
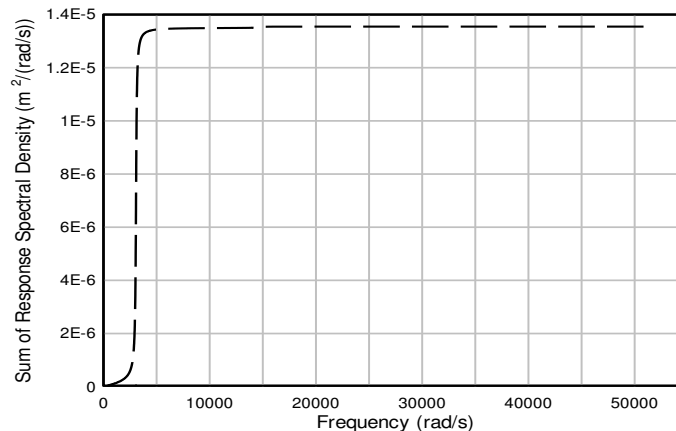
Figure 5. Integration of spectral density function.
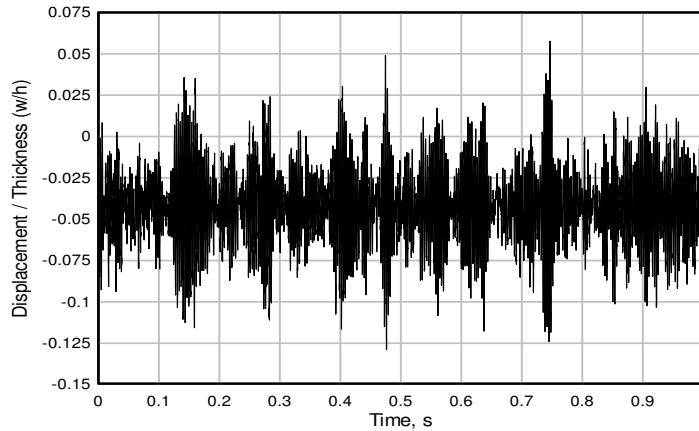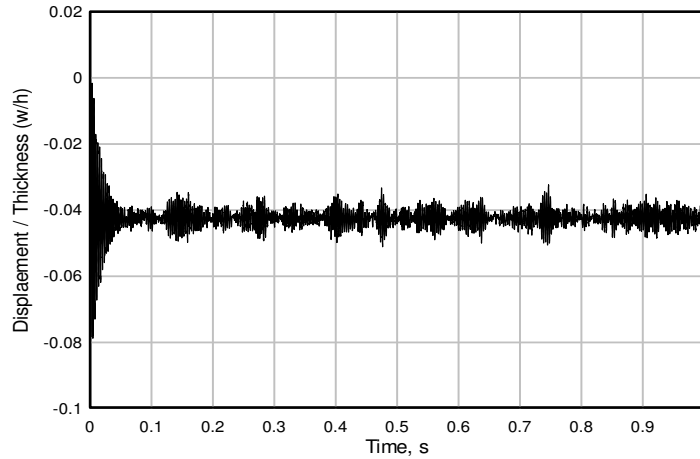
Figure 6. Displacement time history for uniform elevated temperature ($\Delta T = 300\,\text{K}$) and random pressure (SPL $= 160\,\text{dB}$ and $n = 0.7$).

The deflection response for random pressure of SPL $= 160\,\text{dB}$ at the uniformly elevated temperature throughout the plate ($\Delta T = 300\,\text{K}$) is presented in Figure 6. As can be seen from the figure, temperature rise in the inhomogeneous FGM plate with movable ends causes the plate to bend, and consequently, the mean value of the vibration is no longer zero. The plate first is bent due to elevated temperature to MEAN$/h = -0.0424$, and then it continues to vibrate about this mean value with RMS$/h = 0.049$ due to the random pressure.

Similar behavior is seen under the linearly varying temperature through thickness at the same random pressure (SPL $= 160\,\text{dB}$) as displayed in Figure 7. In this case, temperature at the top face of the plate is $T_t = 850\,\text{K}$ and temperature at the bottom face of the plate is $T_b = 350\,\text{K}$, and temperature variation from top to bottom is linear with ambient temperature $T_0 = 300\,\text{K}$. In this case too, the plate bends due to temperature rise in the inhomogeneous FGM plate to a new position where it continues to vibrate randomly. The response averages are MEAN$/h = -0.0086$ and RMS$/h = 0.024$.
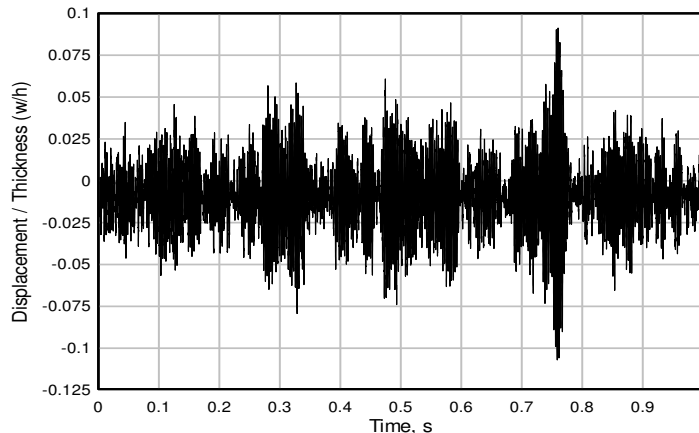
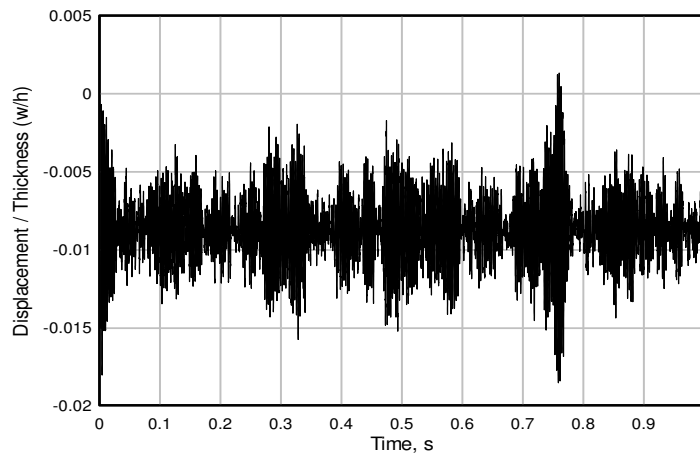**Figure 7.** Displacement time history for linear temperature rise ($T_{\text{top}} = 850\,\text{K}$ and $T_b = 350\,\text{K}$) and uniform random pressure (SPL $= 160\,\text{dB}$, $n = 0.7$ and $T_0 = 300\,\text{K}$).

Figure 8. Displacement time history for uniform elevated temperature ($\Delta T = 300$ K) and random pressure (SPL $= 140$ dB and $n = 0.7$).

The displacement response history of the FGM plate under the random pressure (SPL $= 140$ dB) at uniformly elevated temperature ($\Delta T = 300$ K) is illustrated in Figure 8. In this case, the temperature rise is the same, but random pressure is lower compared to Figure 6. Therefore, the mean deflection response of the FGM plate is the same, but the amplitudes of the random vibration are much smaller. It turns to be like a static response as time goes. Similar behavior, but to a lesser degree, is observed for linearly varying temperature rise as shown in Figure 9. This can be realized by comparing Figures 7 and 9. It is obvious that the response is dominated by the thermal deflections when the random load density is low.

The deflection average responses of the FGM plate under different random loading at different uniformly elevated temperature are plotted in Figure 10. For without thermal effect, the mean response is almost zero, and the RMS value varies linearly with random sound pressure level as is expected for

Figure 9. Displacement time history for linear temperature rise ($T_{\text{top}} = 850$ K and $T_b = 350$ K) and uniform random pressure (SPL $= 140$ dB, $n = 0.7$ and $T_0 = 300$ K).
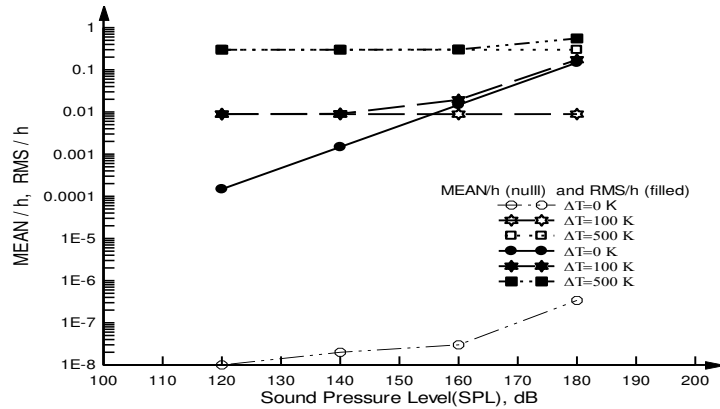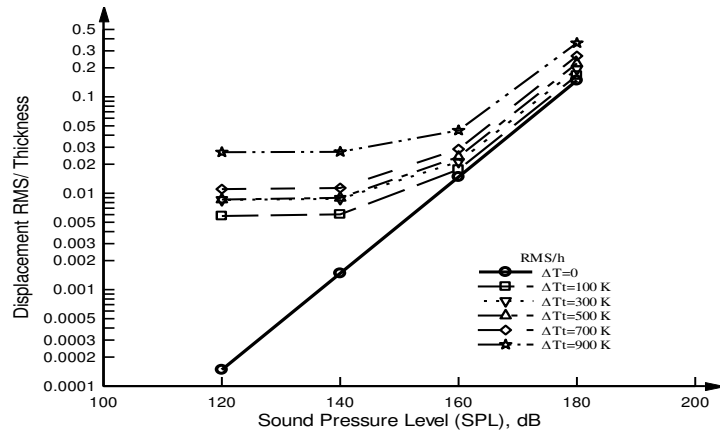
Figure 10. Deflection RMS and MEAN values versus sound pressure levels at different uniformly elevated temperatures ($n = 0.7$).

a linear structure. For other elevated temperature cases, when the SPL is less than 140 dB, thermal deflection dominates the response with the mean. However, random loading response turns out to be predominant after SPL = 140 dB at $\Delta T = 100$ K and after SPL = 160 dB at $\Delta T = 500$ K.

Similar RMS responses are obtained for linearly elevated temperatures as shown in Figure 11. The bottom temperature is kept constant at $T_b = 350$ K, and the top temperature is elevated from the ambient temperature (i.e., $\Delta T_t = T_t - T_0$). The results reveal that the RMS responses increase for all linearly elevated temperatures when the sound pressure level is greater than 140 dB.

The effect of the material distribution parameter n on the RMS/h response under random pressure without thermal influence is presented in Table 2. Both the Monte Carlo method and spectral density method results are tabulated. It is obvious that the two methods agree quite well. The FGM plate transforms from the ceramic-rich plate to the metal-rich plate with increased material distribution parameter n. Consequently, it yields greater RMS responses.

Figure 11. Deflection RMS values versus sound pressure levels at different linearly elevated temperatures ($n = 0.7$).

Method	SPL	$n = 0.1$	$n = 0.5$	$n = 1$	$n = 5$	$n = 10$
Monte Carlo	160 dB	0.0130	0.0143	0.0152	0.0167	0.0172
Spectral density	160 dB	0.0129	0.0143	0.0151	0.0166	0.0172
Monte Carlo	180 dB	0.1302	0.1434	0.1523	0.1675	0.1728
Spectral density	180 dB	0.1296	0.1430	0.1517	0.1669	0.1729

Table 2. The effect of the material distribution parameter n on the RMS/h response ($\Delta T = 0$).

The effect of the material distribution parameter n on the nondimensional RMS and MEAN responses under random loading in a thermal environment is given in Table 3. Temperature distribution through thickness is assumed to be linear with $T_t = 850$ K and $T_b = 350$ K. The mean responses are due to temperature since MEAN responses are almost the same for SPL $= 160$ dB and SPL $= 180$ dB for each n value. The RMS values increase with increased n values as the FGM plate becomes more metal-rich.

The effect of the plate thickness to random response for SPL $= 160$ dB is presented in Table 4. Isothermal, uniformly elevated temperature and linearly elevated temperature cases are considered. For the isothermal vibration case, MEAN responses are zero, and the RMS responses increase with the length-to-thickness ratio. For vibration in a thermal environment, when the plate is very thick (e.g., $a/h = 5$), the response is mainly MEAN response due to elevated temperature, and fluctuations about the mean response due to random loading is very small. When the FGM plate is moderately thick, fluctuations become relatively important for the linearly elevated temperature case but not important for uniformly elevated temperatures.

Sound pressure		$n = 0.1$	$n = 0.5$	$n = 1$	$n = 5$	$n = 10$
160 dB	RMS/h	0.0218	0.0215	0.0271	0.0285	0.0306
	MEAN/h	0.0114	−0.0034	−0.0139	−0.0079	0.0089
180 dB	RMS/h	0.1868	0.2129	0.2325	0.2739	0.2926
	MEAN/h	0.0115	−0.0034	−0.0138	−0.0079	0.0089

Table 3. The effect of the material distribution parameter n on the response averages for linearly elevated temperature.

		$a/h = 5$	$a/h = 10$	$a/h = 20$
Isothermal	RMS/h	0.000132	0.00134	0.0148
$\Delta T = 0$ K	MEAN/h	0	0	0
Uniform temperature rise	RMS/h	0.00127	0.00596	0.04893
$\Delta T = 300$ K	MEAN/h	−0.00126	−0.00571	−0.04238
Linear temperature rise	RMS/h	0.00036	0.00218	0.02326
$T_t = 850$ K, $T_b = 350$ K	MEAN/h	−0.00033	−0.00146	−0.00861

Table 4. Random responses of the FGM plates with various length-to-thickness ratios ($n = 0.7$ and $a = 0.5$ m).
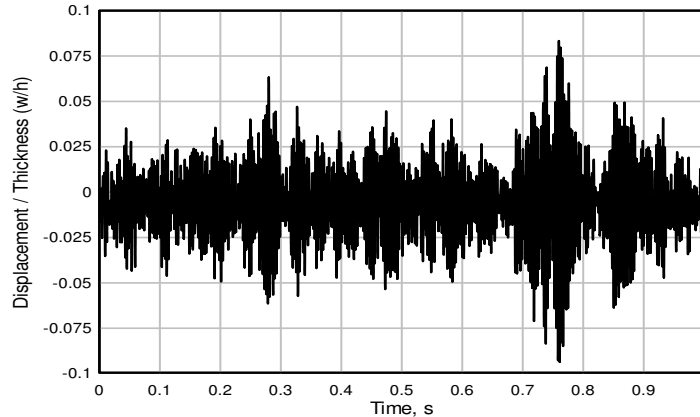
Figure 12. Displacement time history for nonlinear temperature rise ($T_t = 850$ K and $T_b = 350$ K) and random pressure (SPL $= 160$ dB, $n = 0.7$ and $T_0 = 300$ K).

Random response with nonlinear temperature distribution across the thickness is shown in Figure 12. In this case, temperatures of the top and bottom faces are taken to be the same as in the linear temperature distribution case shown in Figure 6. That is, temperature at the top face of the plate is $T_t = 850$ K and temperature at the bottom face of the plate is $T_b = 350$ K, and temperature variation from top to bottom is nonlinear with ambient temperature $T_0 = 300$ K, $k_b = 6.112$ W/mK and $k_t = 1.775$ W/mK in Figure 12. The response averages are found as MEAN$/h = -0.0058$ and RMS$/h = 0.021$. It can be seen that random deflection responses for linear temperature distribution (Figure 7) and nonlinear temperature distribution (Figure 12) across the plate thickness are nearly identical. It is clear that the nonlinear temperature distribution on the random response has no pronounced effect.

5. Conclusion

The transverse vibration of the functionally graded material plates under random excitation is presented. The first-order shear deformation (FSDT) plate theory is used for the equation of motion. The FGM plates are assumed as ceramic-metal mixtures, and their mechanical properties vary exponentially through the thickness. All mechanical properties of the constituents are also considered temperature-dependent. Both the spectral density method (frequency domain) and Monte Carlo method (time domain) are used for investigation. It was found that when the input is uniformly distributed random pressure with zero mean in an isothermal environment, the response is also random with zero mean. Both methods predict the same average values (RMS and MEAN). It was shown that contribution to the random response is mostly coming from the first mode. Therefore, a good estimate can be done by considering the fundamental mode only. Temperature and distribution of temperature also significantly affect the response, particularly the MEAN response. The effect of the material distribution parameter is investigated. When the FGM plate becomes metal-rich ($n > 1$), deflection responses become greater. Influence of the length-to-thickness ratio is also investigated. It was shown that when the FGM plate is very thick, the RMS response to acoustic random pressure is very small. The effect of temperature is found only on the mean responses.

Appendix A

The elements of the stiffness matrix $[K] = [k_{ij}]$ are

$$k_{11} = A_{11}\alpha_m^2 + A_{66}\beta_n^2, \tag{A-1}$$

$$k_{12} = (A_{12} + A_{66})\alpha_m\beta_n, \tag{A-2}$$

$$k_{13} = 0, \tag{A-3}$$

$$k_{14} = B_{11}\alpha_m^2 + nB_{66}\beta_n^2, \tag{A-4}$$

$$k_{15} = (B_{12} + B_{66})\alpha_m\beta_n, \tag{A-5}$$

$$k_{22} = A_{22}\beta_n^2 + A_{66}\alpha_m^2, \tag{A-6}$$

$$k_{23} = 0, \tag{A-7}$$

$$k_{24} = (B_{12} + B_{66})\alpha_m\beta_n, \tag{A-8}$$

$$k_{25} = B_{22}\beta_n^2 + B_{66}\alpha_m^2, \tag{A-9}$$

$$k_{33} = \kappa(A_{55}\alpha_m^2 + A_{44}\beta_n^2), \tag{A-10}$$

$$k_{34} = \kappa A_{55}\alpha_m, \tag{A-11}$$

$$k_{35} = \kappa A_{44}\beta_n, \tag{A-12}$$

$$k_{44} = D_{11}\alpha_m^2 + D_{66}\beta_n^2 + \kappa A_{55}, \tag{A-13}$$

$$k_{45} = (D_{12} + D_{66})\alpha_m\beta_n, \tag{A-14}$$

$$k_{55} = D_{22}\beta_n^2 + D_{66}\alpha_m^2 + \kappa A_{44}. \tag{A-15}$$

The elements of the mass matrix $[M] = [m_{ij}]$ are

$$m_{11} = m_{22} = m_{33} = I_0, \tag{A-16}$$

$$m_{44} = m_{55} = I_2, \tag{A-17}$$

$$m_{14} = m_{25} = I_1. \tag{A-18}$$

Others are zero.

Appendix B

The coefficients γ_1, γ_2, ξ_1 and ξ_2 are defined as

$$\gamma_1(k, r, m) = \frac{a}{4\pi}\left\{ \frac{1}{k+r+m}((-1)^{k+r+m} - 1) - \frac{1}{k+r-m}((-1)^{k+r-m} - 1) \right.$$
$$\left. - \frac{1}{k-r+m}((-1)^{k-r+m} - 1) + \frac{1}{k+r+m}((-1)^{k+r+m} - 1) \right\}, \tag{B-1}$$

$$\gamma_2(k, r, m) = \frac{a}{4\pi}\left\{ \frac{-1}{k+r+m}((-1)^{k+r+m} - 1) + \frac{1}{k+r-m}((-1)^{k+r-m} - 1) \right.$$
$$\left. - \frac{1}{k-r+m}((-1)^{k-r+m} - 1) + \frac{1}{k-r-m}((-1)^{k-r-m} - 1) \right\}, \tag{B-2}$$

$$\xi_1(l, s, n) = \frac{b}{4\pi}\left\{\frac{1}{l+s+n}((-1)^{l+s+n}-1) - \frac{1}{l+s-n}((-1)^{l+s-n}-1)\right.$$
$$\left. - \frac{1}{l-s+n}((-1)^{l-s+n}-1) + \frac{1}{l+s+n}((-1)^{l+s+n}-1)\right\}, \quad \text{(B-3)}$$

$$\xi_2(l, s, n) = \frac{b}{4\pi}\left\{\frac{-1}{l+s+n}((-1)^{l+s+n}-1) + \frac{1}{l+s-n}((-1)^{l+s-n}-1)\right.$$
$$\left. - \frac{1}{l-s+n}((-1)^{l-s+n}-1) + \frac{1}{l+s+n}((-1)^{l+s+n}-1)\right\}. \quad \text{(B-4)}$$

References

[Alijani et al. 2011] F. Alijani, F. Bakhtiari-Nejad, and M. Amabili, "Nonlinear vibrations of FGM rectangular plates in thermal environments", *Nonlinear Dyn.* **66**:3 (2011), 251–270.

[Cederbaum et al. 1992] G. Cederbaum, I. Elishakoff, J. Aboudi, and L. Librescu, *Random vibration and reliability of composite structures*, Technomic Publishing Co., Lancaster, PA, 1992.

[Efraim 2011] E. Efraim, "Accurate formula for determination of natural frequencies of FGM plates basing on frequencies of isotropic plates", *Proc. Eng.* **10**:0 (2011), 242–247.

[Efraim and Eisenberger 2007] E. Efraim and M. Eisenberger, "Exact vibration analysis of variable thickness thick annular isotropic and FGM plates", *J. Sound Vib.* **299**:4–5 (2007), 720–738.

[Elishakoff 1999] I. Elishakoff, *Probabilistic theory of structures*, 2nd ed., Dover, New York, 1999.

[Elishakoff and Gentilini 2005] I. Elishakoff and C. Gentilini, "Three-dimensional flexure of rectangular plates made of functionally graded materials", *J. Appl. Mech.* (*ASME*) **72**:5 (2005), 788–791.

[Fakhari et al. 2011] V. Fakhari, A. Ohadi, and P. Yousefian, "Nonlinear free and forced vibration behavior of functionally graded plate with piezoelectric layers in thermal environment", *Compos. Struct.* **93**:9 (2011), 2310–2321.

[Ghannadpour et al. 2012] S. A. M. Ghannadpour, H. R. Ovesy, and M. Nassirnia, "Buckling analysis of functionally graded plates under thermal loadings using the finite strip method", *Comput. Struct.* **108–109**:0 (2012), 93–99.

[Hasheminejad and Gheshlaghi 2012] S. M. Hasheminejad and B. Gheshlaghi, "Three-dimensional elastodynamic solution for an arbitrary thick FGM rectangular plate resting on a two parameter viscoelastic foundation", *Compos. Struct.* **94**:9 (2012), 2746–2755.

[Hosseini and Fazelzadeh 2010] M. Hosseini and S. A. Fazelzadeh, "Aerothermoelastic post-critical and vibration analysis of temperature-dependent functionally graded panels", *J. Therm. Stresses* **33**:12 (2010), 1188–1212.

[Hosseini-Hashemi et al. 2010] Sh. Hosseini-Hashemi, H. R. D. Taher, H. Akhavan, and M. Omidi, "Free vibration of functionally graded rectangular plates using first-order shear deformation plate theory", *Appl. Math. Model.* **34**:5 (2010), 1276–1291.

[Huang and Shen 2004] X.-L. Huang and H.-S. Shen, "Nonlinear vibration and dynamic response of functionally graded plates in thermal environments", *Int. J. Solids Struct.* **41**:9–10 (2004), 2403–2427.

[Javaheri and Eslami 2002] R. Javaheri and M. R. Eslami, "Thermal buckling of functionally graded plates", *AIAA J.* **40**:1 (2002), 162–169.

[Koizumi 1997] M. Koizumi, "FGM activities in Japan", *Compos. B Eng.* **28**:1–2 (1997), 1–4.

[Lee et al. 2010] Y. Y. Lee, X. Zhao, and J. N. Reddy, "Postbuckling analysis of functionally graded plates subject to compressive and thermal loads", *Comput. Methods Appl. Mech. Eng.* **199**:25-28 (2010), 1645–1653.

[Lin 1976] Y.-K. Lin, *Probabilistic theory of structural dynamics*, Robert E. Krieger Publishing Co., Huntington, NY, 1976.

[Mantari and Soares 2012] J. L. Mantari and C. G. Soares, "Bending analysis of thick exponentially graded plates using a new trigonometric higher order shear deformation theory", *Compos. Struct.* **94**:6 (2012), 1991–2000.

[Maymon 1998] G. Maymon, *Some engineering applications in random vibrations and random structures*, Progress in Astronautics and Aeronautics **178**, American Institute of Aeronautics and Astronautics, Reston, VA, 1998.

[Mohammadi et al. 2010] M. Mohammadi, A. R. Saidi, and E. Jomehzadeh, "Levy solution for buckling analysis of functionally graded rectangular plates", *Appl. Compos. Mater.* **17**:2 (2010), 81–93.

[Nguyen-Xuan et al. 2012] H. Nguyen-Xuan, L. V. Tran, C. H. Thai, and T. Nguyen-Thoi, "Analysis of functionally graded plates by an efficient finite element method with node-based strain smoothing", *Thin-Walled Struct.* **54** (2012), 1–18.

[Prakash et al. 2012] T. Prakash, M. K. Singha, and M. Ganapathi, "A finite element study on the large amplitude flexural vibration characteristics of FGM plates under aerodynamic load", *Int. J. Non-Linear Mech.* **47**:5 (2012), 439–447.

[Praveen and Reddy 1998] G. N. Praveen and J. N. Reddy, "Nonlinear transient thermoelastic analysis of functionally graded ceramic-metal plates", *Int. J. Solids Struct.* **35**:33 (1998), 4457–4476.

[Praveen et al. 1999] G. N. Praveen, C. D. Chin, and J. N. Reddy, "Thermoelastic analysis of functionally graded ceramic–metal cylinder", *J. Eng. Mech.* (*ASCE*) **125**:11 (1999), 1259–1267.

[Reddy 2000] J. N. Reddy, "Analysis of functionally graded plates", *Int. J. Numer. Methods Eng.* **47**:1–3 (2000), 663–684.

[Reddy 2004] J. N. Reddy, *Mechanics of laminated composite plates and shells: theory and analysis*, 2nd ed., CRC Press, Boca Raton, FL, 2004.

[Reddy and Chin 1998] J. N. Reddy and C. D. Chin, "Thermomechanical analysis of functionally graded cylinders and plates", *J. Therm. Stresses* **21**:6 (1998), 593–626.

[Shen 2009] H.-S. Shen, *Functionally graded materials: nonlinear analysis of plates and shells*, CRC Press, Boca Raton, FL, 2009.

[Shen and Wang 2012] H.-S. Shen and Z.-X. Wang, "Assessment of Voigt and Mori–Tanaka models for vibration analysis of functionally graded plates", *Compos. Struct.* **94**:7 (2012), 2197–2208.

[Shinozuka and Jan 1972] M. Shinozuka and C.-M. Jan, "Digital simulation of random processes and its applications", *J. Sound Vib.* **25**:1 (1972), 111–128.

[Thai and Choi 2012] H.-T. Thai and D.-H. Choi, "A refined shear deformation theory for free vibration of functionally graded plates on elastic foundation", *Compos. B Eng.* **43**:5 (2012), 2335–2347.

[Yang and Gao 2013] Q. Yang and C.-F. Gao, "Dynamic stress analysis of a functionally graded material plate with a circular hole", *Meccanica* (*Milano*) **48**:1 (2013), 91–101.

[Yang and Shen 2002] J. Yang and H.-S. Shen, "Vibration characteristics and transient response of shear-deformable functionally graded plates in thermal environments", *J. Sound Vib.* **255**:3 (2002), 579–602.

[Yang and Shen 2003] J. Yang and H.-S. Shen, "Nonlinear bending analysis of shear deformable functionally graded plates subjected to thermo-mechanical loads under various boundary conditions", *Compos. B Eng.* **34**:2 (2003), 103–115.

[Zhang et al. 2012] W. Zhang, Y. Hao, X. Guo, and L. Chen, "Complicated nonlinear responses of a simply supported FGM rectangular plate under combined parametric and external excitations", *Meccanica* (*Milano*) **47**:4 (2012), 985–1014.

[Zhao et al. 2009] X. Zhao, Y. Y. Lee, and K. M. Liew, "Mechanical and thermal buckling analysis of functionally graded plates", *Compos. Struct.* **90**:2 (2009), 161–171.

VEDAT DOGAN: doganve@itu.edu.tr
Faculty of Aeronautical and Astronautical Engineering, Istanbul Technical University, Maslak, 34469 Istanbul, Turkey

JOURNAL OF MECHANICS OF MATERIALS AND STRUCTURES

msp.org/jomms

Founded by Charles R. Steele and Marie-Louise Steele

Cover photo: Mando Gomez, www.mandolux.com